POLITECNICO DI TORINO
Repository ISTITUZIONALE

Environmental implications of hybrid-electric regional aircraft: emissions and climate change

Original
Environmental implications of hybrid-electric regional aircraft: emissions and climate change / Abu Salem, K., Palaia, G.. - (2024). (34th Congress of the International Council of the Aeronautical Sciences, ICAS 2024 Firenze (ITA) 9-13 September 2024).

Availability:
This version is available at: 11583/2997842 since: 2025-02-25T16:16:26Z

Publisher:
International Council of the Aeronautical Sciences

Published
DOI:

Terms of use:

This article is made available under terms and conditions as specified in the corresponding bibliographic description in the repository

Publisher copyright

(Article begins on next page)

26 November 2026



Environmental implications of hybrid-electric regional aircraft: emissions and climate change

Karim Abu Salem[1a], Giuseppe Palaia[1b]

[1]Mul2 Group, Department of Mechanical and Aerospace Engineering, Politecnico di Torino, Corso Duca degli Abruzzi 24, Torino, Italy

[a]*karim.abusalem@polito.it* [b]*giuseppe.palaia@polito.it*

Abstract

This paper presents a performance analysis of hybrid-electric aircraft focused on emissions estimation. Specifically, the aim is to provide a broad overview of emissions reduction potential and the environmental impact related to the introduction of hybrid-electric propulsion in the regional sector. The discussion, based on outcomes of conceptual studies and information available in the literature, aims to provide a qualitative picture that highlights both the potential gains and the critical issues connected with the practical technological utilization of hybrid-electric propulsion for regional aircraft, and its general implications on environmental issues. The conceptual design of the hybrid-electric aircraft was carried out using an in-house multidisciplinary optimization framework, whereas the 'Boeing fuel flow method 2' was used to estimate pollutant emissions. The paper is divided into two parts: the first part is aimed at comparing the non-CO_2 emissions, i.e. NO_x, HC, SO_2, CO, of a hybrid-electric aircraft designed to minimize block fuel, with a thermal aircraft designed by the same methodology and according to same requirements; the second part presents a similar assessment but focusing on CO_2 emissions. The CO_2 assessment takes both flight and electricity generation emissions into account. The results of the first part show that the hybrid-electric configuration could provide room for non-CO_2 emissions reduction, both during the entire mission the landing and take-off cycle. However, further refinement of predictive models for emissions computation are needed to improve these predictions. The results of the second part show that the hybrid-electric configuration could provide CO_2 emissions reductions for design ranges below 600 nm; however, if the ground electric energy production does not shift towards a full renewable-based scenario, these benefits could result marginal.

Keywords: hybrid-electric; regional aircraft; aircraft design; mission performance; green aviation; environmental impact; emissions.

1. Introduction

The development of hybrid-electric propulsion for transport aircraft applications has gained considerable relevance in the context of aerospace research [1],[2]. This propulsion technology has the potential to reduce, even significantly, the pollutant emissions directly related to flight, and thus to mitigate the environmental impact of aviation. This potential benefit, however, comes up against some practical challenges that are somewhat constraining the effective application of this technology on transport aircraft; among these, there are the integration of electric components on the aircraft [3], the consistent assessment of reliability and safety [4],[5], the compatibility with infrastructures [6],[7], and above all, the actual possibility to push forward the technological maturity of the main electric components of the powertrain. This last aspect is of paramount importance even during the conceptual assessment of hybrid-electric aircraft; in particular, the technological development of batteries is a key enabler for the effective application of hybrid-electric propulsion on aircraft, and the current low gravimetric energy density of such components is a major showstopper [8],[9]. Even the most optimistic forecasts of an increase in battery technology maturity do not suggest that hybrid-electric propulsion can be used beneficially on aircraft larger than those typically operated in the regional category [10]. In fact, the weight increases related to the amount of batteries to be installed on board would introduce penalizations that affect the overall aircraft performance, even undermining its feasibility. Unless non-evolutionary breakthroughs are achieved in the field of electric energy storage systems, an actual application of hybrid-electric propulsion for the coming decades will therefore only involve aircraft with limited range and payload, reasonably no more than 800 nm and 80 passengers, in line with the current regional turboprop aircraft market [11],[12].

This paper aims to provide a general and qualitative discussion of the potential environmental benefits resulting from the utilization of regional hybrid-electric aircraft. Specifically, the presented discussion is structured on two different levels regarding two distinct issues arising from the flight-related emissions: local air quality degradation and climate change. The first issue relates primarily to air pollution associated with aircraft operations on the ground and at low altitude, impacting on areas surrounding the airports; such areas may be densely populated. There is evidence that the degradation of air quality in these areas is caused by non-CO_2 emissions (e.g., NO_x, SO_x, particulate matter, etc.) released from aircraft exhausts, and that this phenomenon could significantly impact the quality of life and health of the citizens [13],[14]. The implications of aircraft transport on climate change, on the other hand, are different [15],[16]; in the long term, it is CO_2 emissions that have the main effect on global warming, while there are still uncertainties on the quantification of the impact of non-CO_2 greenhouse gas emissions, and these appear to have effects on a shorter time scale [17],[18]. The assessment of aircraft emissions, already in the conceptual design phase, is useful to preliminary evaluate the impact on global warming, as proposed in refs. [19],[20].

The discussion presented in this paper aims to set the basis for a consistent addressing of: *i)* the impact the conversion of the regional sector to hybrid-electric propulsion would have on emissions; *ii)* the technological and methodological limitations related to the reliable estimations of these assessments. Specifically, a methodology is presented based on conceptual aircraft design procedures together with predictive emission models available in the literature. In order to adequately evaluate the environmental impact of hybrid-electric powertrains, it is necessary to thoroughly characterise pollutant emissions over the entire operating envelope of the aircraft, for both CO_2 and non-CO_2 substances. For turboshafts currently in service on full-thermal regional aircraft, there are databases and related predictive models that allow reasonable estimations of the emissions of these pollutants [21],[22]. However, many current studies show that hybrid-electric powertrains optimised to minimise fuel consumption, for example, may require operating conditions of the thermal power system that are not expected in current standard cases, e.g. low power output or low fuel flow of the thermal engine in some specific flight phases. It is therefore necessary highlight the possible limitations of the emissions prediction models for non-standard turboshaft operations. From a technological perspective, on the other side, it is pointed out that if a sharp conversion of the ground-based electric energy production towards a full renewable scenario is not achieved, just introducing technological advancements as hybrid-electric propulsion may not be sufficient to cut noticeably the CO_2 emissions. The presented discussion, based on outcomes of conceptual studies, information available in the literature, and technological forecasts, aims to provide a qualitative picture that highlights both the potential gains and the critical issues connected to the practical technological development of hybrid-electric propulsion for regional aircraft, and its implications on environmental topics. The paper is organized as follows: Section 2 presents an overview of the methodological frame adopted; Section 3 provides a discussion on the results obtained, for both CO_2 and non-CO_2 emissions assessments, and finally Section 4 gives the conclusion.

2. Material and Methods

This section outlines the methods and the tools used to reach the outcomes supporting the discussion provided in this paper. Specifically, Section 2.1 outlines the assumptions and the requirements steering the conceptual design of the regional aircraft; Section 2.2 briefly describes the conceptual design framework developed to size and analyse hybrid-electric regional aircraft. Sections 2.3 and 2.4 provide a description of the models used to compute the emissions, both CO_2 and non-CO_2, deriving from the operation of a turboshaft engine; this internal combustion unit is the one considered for the application in parallel hybrid-electric powertrains. The CO_2 emissions deriving from the electricity production to charge the aircraft battery is also taken into account.

2.1 Preliminaries and assumptions

The research is focused on the conceptual design and performance analysis of a regional aircraft. The regional transport category is the most realistically suitable among transport aircraft for integrating hybrid-electric propulsion [2]. Hence, in this conceptual study the aircraft design requirements are set similar to those of the turbopropeller-powered ATR 42, namely a regional aircraft capable of transporting 40 passengers over a design distance varying between 200 and 600; the cruise Mach is set equal to 0.4 and the cruise altitude is 6096 m. The aircraft's two propellers are powered by hybrid-electric powertrains with parallel architecture; this architecture allows the thermal and electric sources

to supply power to the propeller independently. The electric motor and the thermal engine are linked to the propeller by a gearbox. An artistic view of such an aircraft, equipped with turboprop engines, is shown in Figure 1. Considering an entry into service beyond 2035, the electric powertrain component main performances are: battery energy density (BED) at pack level = 500 Wh/kg, and electric motor power density = 15 kW/kg. Details on the requirements and assumptions on the set-up of the aircraft design process are available in ref. [2].



Figure 1. Artistic view of the considered regional aircraft

2.2 Hybrid-electric aircraft design

The conceptual design and performance analysis methodology for hybrid-electric aircraft is implemented in the in-house developed software THEA-CODE [23]. This code allows the overall design of hybrid-electric aircraft by integrating the main interdisciplinary features typical of the conceptual stage of aircraft design process. As the purpose of this paper is to discuss the environmental impact of the utilization of hybrid-electric regional aircraft, only a brief introduction of the design methodology is provided; for a more detailed understating of the methodology used, the reader can refer to [2],[23]-[24]. The code performs the sizing of hybrid-electric aircraft starting from a set of TLARs; the initial lifting system geometry is provided as an input, deriving from an in-house developed aerodynamic design code, named AEROSTATE (see [25],[26]). Next, the configuration passes through an iterative loop based on the convergence of the Maximum Take-Off Weight (MTOW). In the loop, schematically represented in Figure 2, different multidisciplinary analyses are consecutively performed. The aerodynamic performance, considering lift coefficient, induced drag, and stability derivatives, is evaluated through vortex lattice method VLM solver (see [27]), whereas the parasitic drag is assessed by means of literature models [28] and results obtained from XFOIL code [29]. The structural weight of the lifting system is evaluated by means of FEM-based surrogate models, as described in [30],[31]. The weights of fuselage, landing gear, secondary structures, on-board systems, and cabin furnishings, are computed through the semi-empirical models reported in [32]. The hybrid-electric powertrain is sized by building the matching chart, a diagram that relates the aircraft wing loading W/S and the specific power P/W required for the different stages of the mission, see [33],[34]. The split of the installed power between the electric and thermal chains is set by the hybridisation factor H_P, that is a design variable defined as:

$$H_P = \frac{P_i^e}{P_i^e + P_i^t} \tag{1}$$

where P_i^e is the installed electric power and P_i^t is the installed thermal power. Following these multidisciplinary evaluations, a simulation of the design mission is carried out, by time integrating the point-mass aircraft equations of motions according to the models described in [35]. The outcomes of the mission simulation enable the extrapolation of all flight performance, as the fuel and battery quantities required for the mission and reserves. At this stage, the design loop is iterated until the MTOW converges.

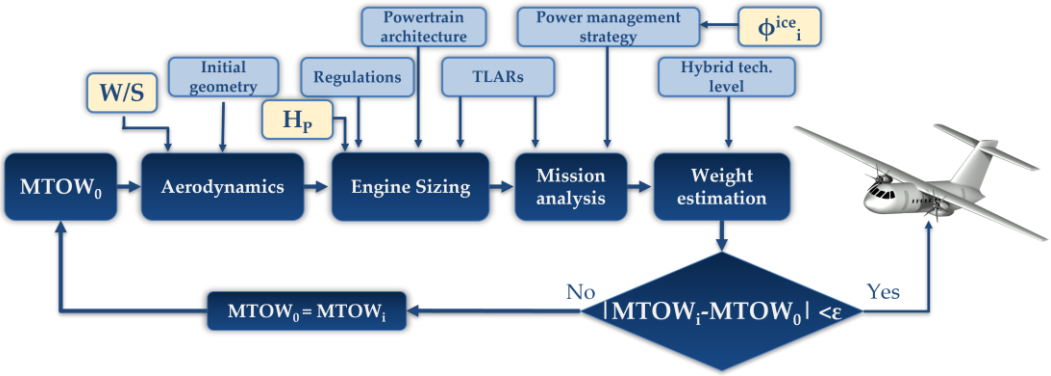

Figure 2. Scheme of the THEA-CODE multidisciplinary aircraft design workflow.

When sizing a hybrid-electric aircraft, establishing a mission power supply strategy is crucial. This strategy must determine the share of power provided by the thermal and electric systems to meet the power demands throughout the flight. In this study, the mission was divided into main sub-segments, and the power supply strategy was defined as follows: during the ground manoeuvre (i.e. taxi-out and taxi-in), only the electric power is used, aiming at minimizing local air pollution and noise; during take-off, both electric and thermal power are utilized to supply maximum available power; for climb, cruise, and descent, the designer can set the ratios of thermal and electric power required to meet the power demands. In this study, the power fractions for these phases, namely Φ^t_{cl}, Φ^t_{cr} and Φ^t_{de}, are determined through an optimization procedure, formalized as follows:

$$\begin{cases} \min(\text{FoM}(\boldsymbol{x})) \\ 0 < H_P < 0.7 \\ 250 < W/S < 325 \\ 0 < \Phi^t_{cl} < 0.56 \\ 0 < \Phi^t_{cr} < 0.56 \\ 0 < \Phi^t_{de} < 0.56 \\ \Phi^e_k < \Phi^e_{k,max} \end{cases} \tag{2}$$

The optimization, aimed at minimising the selected figure of merit (FoM), relies on a multi-start approach, which employs gradient-based optimum search algorithms for each considered starting point. The optimiser can manage the electric power share installed on board through the H_P design variable, and can also search for the best power split supply strategy for the mission, by acting on the fraction of supplied thermal power Φ^t_k, defined as:

$$\Phi^t_k = \frac{P^t_k}{P^t_i} \tag{3}$$

where P^t_k represents the thermal power supplied in the *k-th* mission phase. Considering a parallel powertrain architecture, knowing Φ^t_k it is also possible to compute Φ^e_k, i.e., the electric power fraction supplied in the same phase, as the total required power at each instant of the flight is known from the mission simulation module. The diversion phase, that is to be considered in the sizing process of a transport aircraft, is fixed by the designer to be carried out only with thermal power; indeed, diversion impacts on the aircraft and powertrain sizing, but is only completed in very occasional cases of emergencies or unforeseen occurrences. Hence, this design choice allows to prevent installing heavier battery pack that are left unused in standard operations and having a snowball effect on the aircraft MTOW, affecting its feasibility and effectiveness. Figure 3 reports a generic example of the mission time profile of the thermal and electric power supply for a regional hybrid-electric aircraft and the corresponding thermal and electric power fractions Φ.

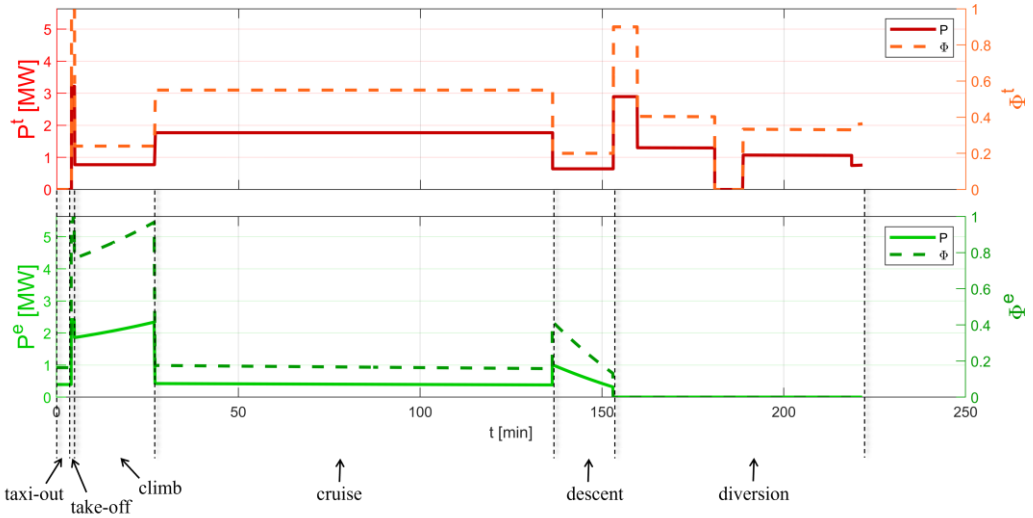

Figure 3. Example of a flight time-profile of the thermal (top) and electric (bottom) power supply.

2.3 Non-CO_2 emissions assessment

The proposed method allows for the calculation of emissions of a commercial transport aircraft during the ground (taxiing and take-off) and airborne (climb, cruise and descent) phases. The methodology has been applied to estimate the main non-CO_2 emissions resulting from engine operations and fuel combustion, namely nitrous oxide NO_x, sulphur dioxide SO_2, hydrocarbons HC, carbon monoxide CO, and water vapour H_2O. The method used in this work estimates the emissions by previously computing the emission index (EI), a parameter that indicates the mass of the pollutant emitted, measured in grams, per unit mass of fuel burned, measured in kilograms. The emissions of SO_2 and H_2O are proportional to fuel flow and therefore have a constant EI, reported in Table 1.

Table 1. EI of H_2O and SO_2

	H_2O	**SO_2**
EI [g/kg]	1237 [36]	1.176 [37]

The estimation of CO, HC and NO_x emissions is based on the Boeing *'fuel flow method 2*' [38][39], which adheres to the scheme shown in Figure 4. Specifically, the following steps are carried out: *i)* extrapolation of flight data such as air density, temperature, and Mach number, *ii)* calculation of the reference fuel flow $\dot{m}_{fr}$, *iii)* calculation of the reference emission index REI, *iv)* calculation of the emission index, *v)* calculation of the emission. The adjective 'reference' refers to the standard atmospheric conditions defined by ICAO, i.e. at sea level and temperature of 15°C.

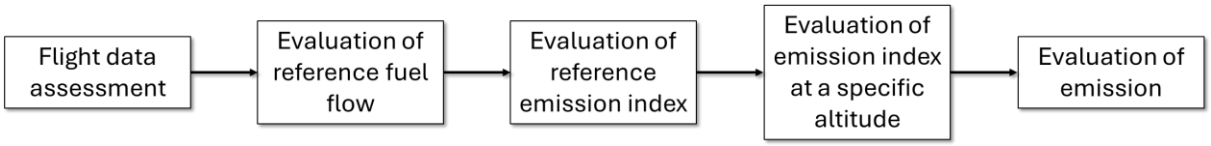

Figure 4. Workflow to assess pollutant emissions

As first step, air pressure, temperature, flight Mach and fuel flow $\dot{m}_f$ are taken from the flight simulation. These data are used as input of the second step, which calculates the reference fuel flow by means of Eq. (4):

$$\dot{m}_{fr} = \dot{m}_f \frac{\theta^{3.8}}{\delta} e^{0.2M^2} \tag{4}$$

where M is the flight Mach, θ is the ratio between the air pressure at the flight altitude and the reference air pressure, δ is the ratio between the air temperature at the flight altitude and the reference air temperature. Figure 5 shows the differences between the fuel flow and the reference fuel flow of the mission described in Section 2.1; the difference between the fuel flows emerges in the airborne phases, i.e. climb, cruise and descent.

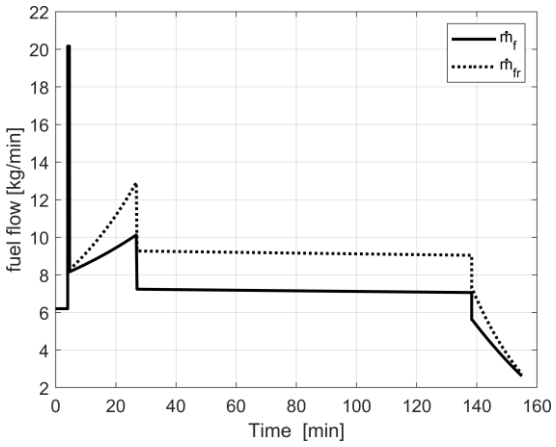

Figure 5. Fuel flow and reference fuel flow vs time

The REI is calculated from engine emission charts that report REI vs. the reference fuel flow (see refs. [38],[39]); these data are typically obtained by the engine manufacturers by means of ground tests on the engine operating at different power levels, ranging from idle (7% of installed power) to take-off (100% of installed power). As an example, Table 2 shows data of the PW127M ground test, a turboshaft used in current regional aircraft.

Table 2. REI of PW127M [40]

Mode	Power [Hp]	$\dot{m}_{fr}$ [kg/min]	REI_{CO} [g/kg]	REI_{NOx} [g/kg]
Nominal idle	192	3.06	9.2	6.9
Approach	825	5.15	3.7	9.8
Max. cruise	2132	8.28	2.2	15.6
Max. climb	2192	8.38	2.0	16.2
Max. continuous power	2475	9.22	2.0	16.5
Take-off	2750	9.90	2.0	17.7

When dealing with the conceptual design of a novel aircraft, the emission curves of potential new engines are not available, and it is necessary to use models from the literature to reasonably estimate the REI. This is even more important when designing hybrid-electric aircraft, that may require thermal engines different that those typically used currently on aircraft of comparable category, and whose predicted emission outputs are not available. The research described in ref. [22] allows, thanks to the analysis of a large turboshaft/turboprop database, to estimate the REI of a wide range of engines already at the conceptual stage. Specifically, ref. [22] establishes that the REI (of CO, HC and NO_x) depends on the engine pressure ratio P_r and the reference fuel flow and, accordingly, defines a mathematical relationship between REI, fuel flow and pressure ratio. This mathematical relationship, which can be represented in the form of a response surface, is generated in case of four different engine operating conditions, namely idle (ID), approach (AP), climb (CL) and take-off (TO), as shown in Figure 6. The fuel flow boundaries for each operating condition, also reported in Table 3, are obtained by varying the reference engine PW127M fuel flow values by ± 5% for each condition.

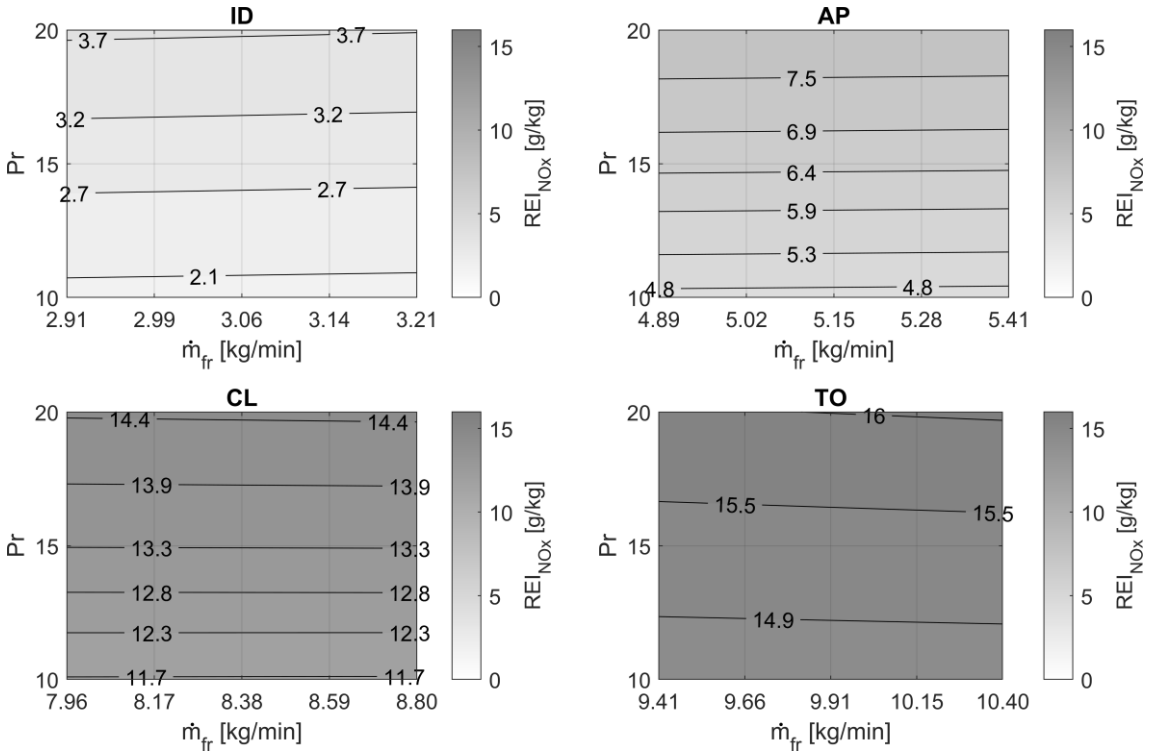

Figure 6. REI of NO_x of four operating configurations (Idle, Approach, Climb and Take-Off) vs reference fuel flow and pressure ratio

Table 3. Maximum and minimum fuel flow values for each engine operating condition

Mode	min($\dot{m}_{fr}$) [kg/min]	max($\dot{m}_{fr}$) [kg/min]
Idle	2.91	3.21
Approach	4.89	5.41
Climb	7.96	8.80
Take-off	9.41	10.40

For the present study case, the value of P_r is set equal to 15, in line with current values for engines used in regional aircraft [22]. Hence, the data extracted from the response surfaces of Figure 6 for the selected value of P_r are plotted on a REI vs. reference fuel flow diagram and an interpolation curve is identified for each pollutant substance. In particular, as reported in [38], it is assumed that CO and HC data are distributed according to an exponential (decreasing) trend, whereas NO_x data are

distributed according to a power function. Accordingly, Eq.s (5,6) has been used to fit the data, and the parameters *a* and *b* are determined by the least square method.

$$REI_{CO\text{-}HC} = a\, e^{-b\dot{m}_{fr}} \tag{5}$$

$$REI_{NO_x} = a\, \dot{m}_{fr}^{b} \tag{6}$$

Figure 7 depicts the fitting curves of Eq. (5,6) together with the data of REI extracted from ref. [22], and Table 4 details the data of the parameters *a* and *b* and the R^2 value.

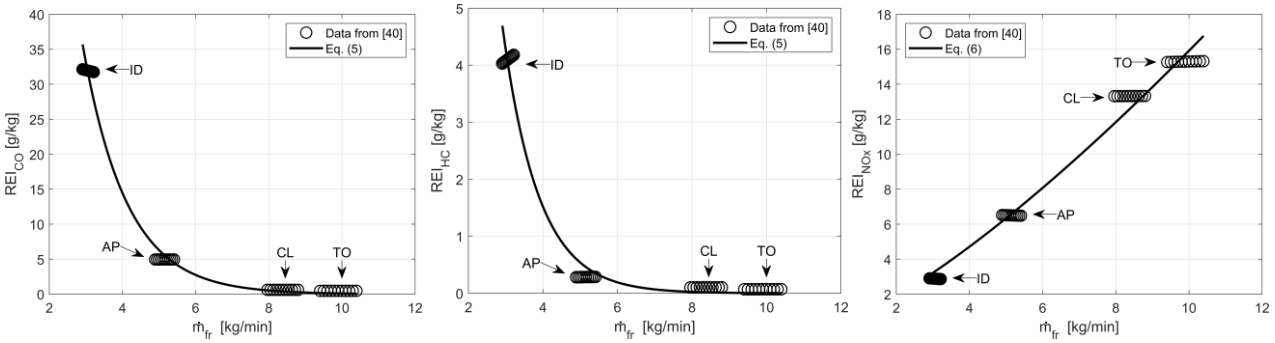

Figure 7. REI vs reference fuel flow of CO (left), HC (centre), NO_x (right)

Table 4. a, b and R^2 values

	CO	HC	NO_x
a	400.8	95.6	0.7473
b	0.8311	1.036	1.328
R^2	0.9896	0.9778	0.9833

According to the selected boundaries for fuel flow, based on data relating to the PW127M, Eq. (5,6) provide the REI value in the case of fuel flow ranging from 2.91 kg/min to 10.40 kg/min. Fuel flow values above or below these limits must be calculated by extrapolating the fitting curves; in particular, as shown in Figure 7, CO and HC REI estimates are not trivial for fuel flows below the lower limit. In fact, if data are extrapolated according to Eq. (5), as shown in Figure 8, we would have a very high REI prediction. Instead, a linear extrapolation shows that fuel flow values below 2.91 kg/min gives an estimation of the REI of CO and HC that seems more plausible; however, a refined model for low values of fuel flow is necessary to rigorously provide reliable assessments. In fact, as stated in [41], special care must be taken when estimating the REI corresponding to fuel flow values at low engine power rating, which could lead to high REI estimate. In this study, a linear extrapolation was assumed.

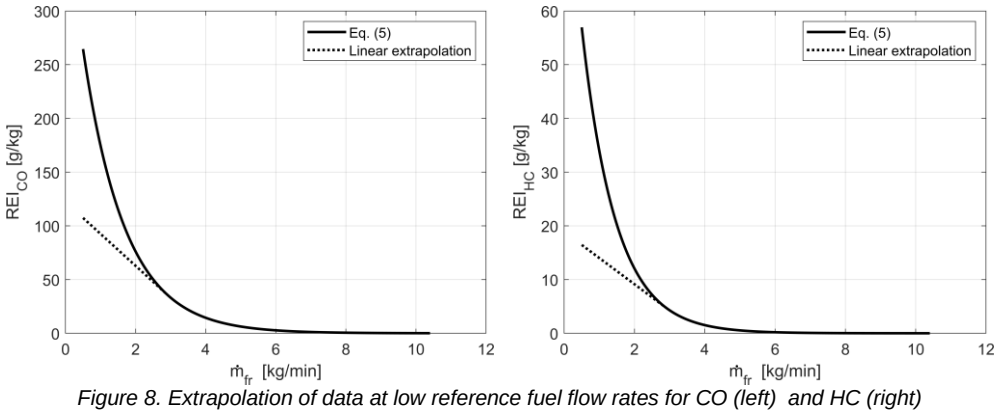

Figure 8. Extrapolation of data at low reference fuel flow rates for CO (left) and HC (right)

The EI value at each time of the mission is now calculated using Eq. (7,8), where *H* is a humidity correction factor. These equations represent the so-called 'Boeing fuel flow method 2', described in detail in ref. [38][39]. The emission is calculated by means of Eq. (9), where *t* is the time extent of the mission.

$$EI_{CO\text{-}HC} = REI_{CO\text{-}HC} \frac{\theta^{3.3}}{\delta^{1.02}} \tag{7}$$

$$EI_{NO_x} = REI_{NO_x} \sqrt{\frac{\delta^{1.02}}{\theta^{3.3}}} e^{H} \quad (8)$$

$$E = \int_0^t EI\, \dot{m}_f dt \quad (9)$$

2.4 CO_2 emissions assessment

The emission of CO_2 (E_{CO_2}) is calculated as follows:

$$E_{CO_2} = EI_{CO_{2_f}} m_{fb} + EI_{CO_{2_e}} m_b (BED/10^3) \quad (10)$$

where $EI_{CO_{2_f}}$ is the mass of CO_2 emitted per kilogram of fuel burned, set equal to 3.16 kg/kg, see [42], and m_{fb} is the block fuel mass. $EI_{CO_{2_e}}$ is the mass of CO_2 emitted per unit of kWh of electricity produced, m_b is the battery mass, and BED is the gravimetric battery energy density. Five different values of $EI_{CO_{2_e}}$ were considered, i.e. {0.42, 0.315, 0.21, 0.105, 0} kg/kWh; the highest value indicates the amount of emission per unit of electric energy production in line with the current energy mix [43], and the other values provide reduced emissions as a growing fraction of energy produced by renewable sources is considered, up to a future scenario in which the whole production is renewable-based, as expected by policies, see [44],[45].

3. Results

This section presents the results of the conceptual assessment of the emissions deriving from hybrid-electric regional aircraft operations, by considering the non-CO_2 (Section 3.1) and the CO_2 (Section 3.2) contributions.

3.1 Non-CO_2 emissions

This section presents the main results obtained using the methodology described in Section 2.2 and selecting the block fuel as objective function to be minimized. Specifically, two different configurations are analysed, one thermal and one hybrid-electric. Both configurations were designed using the same conceptual design code and the same TLARs (see Section 2.1); Table 5 shows the main data of the two configurations, including operating empty weight W_{oe} and payload mass m_p.

Table 5. Main data of hybrid electric and thermal aircraft configuration

Thermal aircraft			**Hybrid-electric aircraft**		
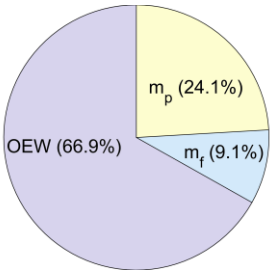	*MTOW* [kg_f]	15781	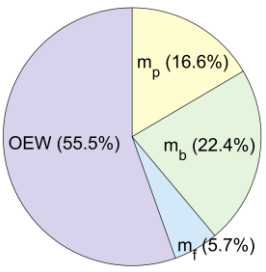	*MTOW* [kg_f]	23000
	W_{oe} [kg_f]	10550		W_{oe} [kg_f]	12753
	m_p [kg]	3800		m_p [kg]	3800
	m_{fb} [kg]	1103		m_{fb} [kg]	872
	m_b [kg]	0		m_b [kg]	5149
	n° pax	40		*n° pax*	40

Figure 9-left shows the comparison of fuel flow throughout the mission between the full-thermal and the hybrid-electric configuration; in particular, hybrid-electric configuration reduces fuel consumption in the climb and descent phases. The detail of fuel flow for ground phases, i.e. taxi-out and take-off, is highlighted in Figure 9-right: the hybrid-electric configuration shows a lower fuel consumption in take-off, and it is completely eliminated in during taxiing phase, as this stage is accomplished only with electric power.

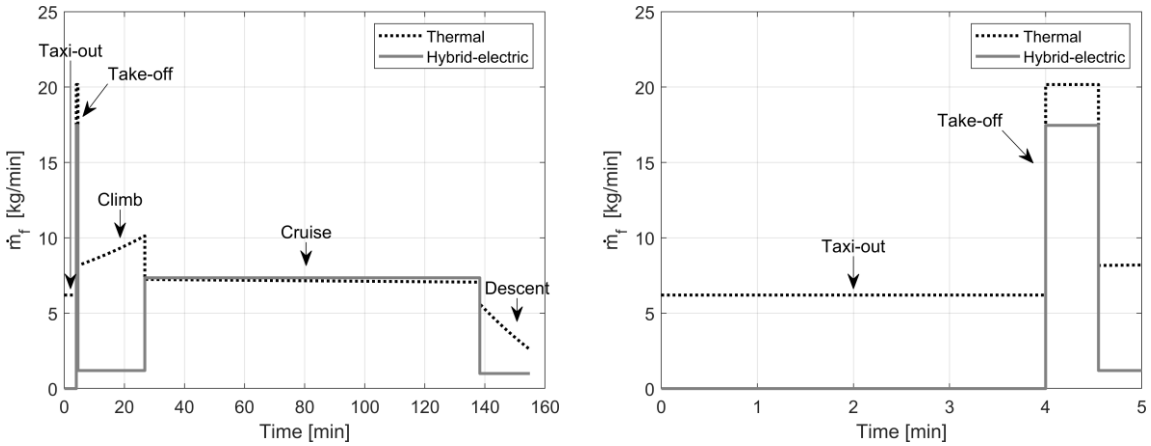

Figure 9. Fuel flow vs. time, profile for the entire mission (left) and zoom on taxi and take-off (right)

The fuel flow directly affects the quantity of emissions; in particular, pollutants such as SO_2 and H_2O (in form of water vapour) have a constant EI with respect to fuel flow, which implies that reductions in fuel consumption are proportional to these emissions. On the other hand, considering HC, CO and NO_x emission indices, it is necessary to take into account how the related EI vary during the phases of the mission. As shown in Figure 7, the trends of the HC and CO curves are opposite to that of NO_x; in fact, reductions in fuel flow generate an increase (reduction) in the REI of HC and CO (NO_x). Figure 10 show how HC, CO and NO_x EI vary in case of the considered test-cases of hybrid-electric and thermal aircraft. The results show that during climb and descent, the lower fuel flow required to the thermal engine of the hybrid-electric powertrain results in higher EI_{HC} and EI_{CO} than the thermal aircraft. The opposite occurs in the case of EI_{NOx}, which results lower for hybrid-electric aircraft. During the cruise phase, the hybrid-electric aircraft burns comparable fuel than the thermal configuration, this a quite similar situation for EI of HC, CO, and NO_x.

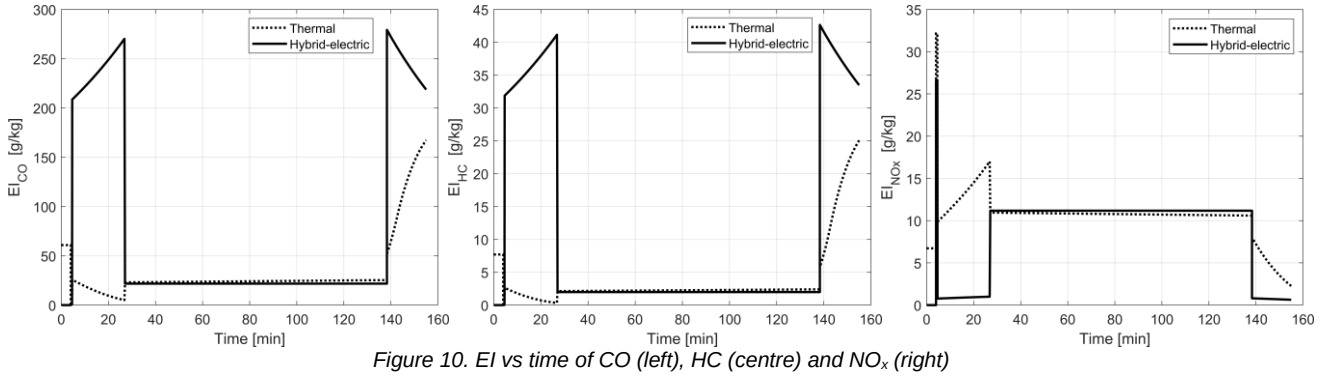

Figure 10. EI vs time of CO (left), HC (centre) and NO_x (right)

Figure 11 depicts the emission rate $\dot{E}$ (i.e. the time derivative of the emission, calculated as reported in Eq. 11) of CO, HC and NO_x throughout the mission. The results qualitatively summarize both the effects of the trends of fuel flow and EI, cf. Figure 9 and Figure 10.

$$\dot{E} = EI\ \dot{m} \tag{11}$$

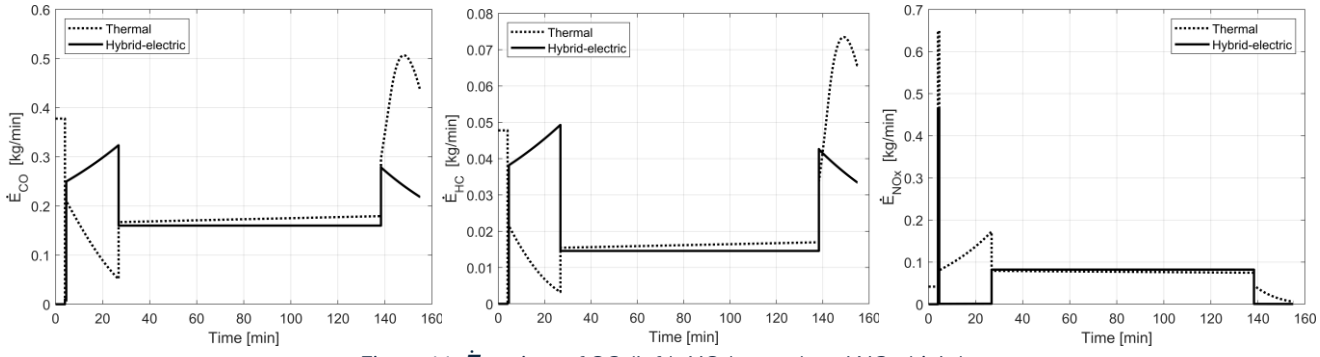

Figure 11. $\dot{E}$ vs time of CO (left), HC (centre) and NOx (right)

The absolute values of fuel consumption and corresponding emissions calculated in each phase of the mission are shown in Table 6. The data show that the hybrid-electric aircraft, thanks to its overall

lower fuel consumption, allows to reduce emissions of all pollutants the whole mission budget is considered. Analysing the mission phase breakdown, it is shown that during the taxiing phase, there is a 100% reduction of emissions, as this phase is accomplished using only the electric propulsion. During the take-off and climb phases, emissions are reduced, except for HC and CO; this is related to the results shown in Figure 11 (left, centre), that highlight the higher emission rate of the hybrid-electric aircraft for these substances; however, in the overall mission budget for these pollutants, the impact of these phases is minor. During the cruise phase, fuel consumption is slightly higher for the hybrid-electric configuration, resulting in increased emissions of pollutants proportional to the fuel flow as SO_2 and H_2O, and increase of NO_x emission, but a reduction in HC and CO emissions. In the descent phase, a reduction of all pollutants is observed. This highlights the fact that although the EI of pollutants such as HC and CO can be higher for the hybrid-electric aircraft (see Figure 10), the lower fuel flow allows a reduction in the overall emission.

Table 6 Emission data of the hybrid electric configuration and the reference thermal aircraft over the entire mission

	Aircraft	Taxi	Take-off	Climb	Cruise	Descent	Total
m_f [kg]	T	24.8	11.1	202	797	68	1103
	HEA	0	9.6	26.6	819	17	872
	Δ	- 24.8	- 1.5	- 175.4	+ 22	- 51	- 231
E_{NO_x} [kg]	T	0.17	0.36	2.67	8.59	0.34	12.1
	HEA	0	0.25	0.02	9.16	0.01	9. 5
	Δ	- 0.17	- 0.09	- 2.65	+ 0.57	- 0.33	- 2.6
E_{HC} [kg]	T	0.19	6e-5	0.24	1.81	1.05	3.29
	HEA	0	2e-4	0.97	1.63	0.63	3.22
	Δ	- 0.19	+ 1.4e-4	- 0.73	- 0.18	- 0.42	- 0.07
E_{CO} [kg]	T	1.5	2e-3	2.74	19.3	7.5	31.1
	HEA	0	5e-3	6.3	17.8	4.1	28.3
	Δ	- 1.5	+ 3e-3	- 3.56	- 1.5	- 3.4	- 2.8
E_{SO_2} [kg]	T	0.03	0.013	0.24	0.94	0.08	1.3
	HEA	0	0.011	0.03	0.96	0.02	1.02
	Δ	- 0.03	- 0.002	- 0.021	+ 0.02	- 0.06	- 0.28
E_{H_2O} [kg]	T	30.7	13.7	250	986	83	1363
	HEA	0	12	33	1014	21	1079
	Δ	- 30.7	- 1.7	- 217	+ 28	- 62	- 284

An important aspect to be analysed is the emission of the take-off and landing (LTO) phase, which includes the taxiing, take-off and climb phase up to an altitude of 915 m [13]. This aspect is of particular interest for the improvement of the so-called local air quality, i.e. the air quality in the surrounding areas of the airport. The data are presented in Table 7 and show that the hybrid-electric aircraft is able to reduce emissions of all pollutants both in the whole mission and in the LTO.

Table 7 Emission data of the hybrid electric configuration and the reference thermal aircraft for LTO

	Aircraft	Mission	LTO
m_f [kg]	T	1103	36
	HEA	872	9.6
	Δ%	-21%	-73.3%
E_{NO_x} [kg]	T	12.1	0.801
	HEA	9.45	0.258
	Δ%	-21.9%	-32.2%
E_{HC} [kg]	T	3.29	0.255
	HEA	3.22	0.126
	Δ%	-2.1%	-50.6%
E_{CO} [kg]	T	31.1	2.151
	HEA	28.3	0.832
	Δ%	-9%	-61.3%
E_{SO_2} [kg]	T	1.3	0.074
	HEA	1.02	0.016
	Δ%	-21%	-78.4%

Some final remarks of the previous discussion; in this study, the emissions of the main pollutants deriving from the combustion of jet fuel into a thermal engine have been estimated. Specifically, the framework developed uses the method proposed by Boeing [38] coupled with the model proposed in ref. [22]. This model was used to compare the emissions of a thermal aircraft and a hybrid-electric aircraft sized using the same design methodology. The results obtained show that the hybrid electric aircraft could provide the room to reduce emissions of all pollutants not only in the whole mission but also in the LTO cycle, as shown in Figure 12.

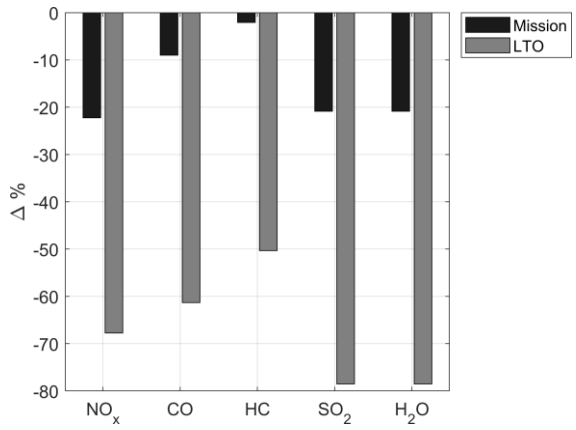

Figure 12. Percentage variation of emission for the design mission and the LTO cycle between hybrid-electric and thermal aircraft

In particular, the strategy of accomplishing the taxiing phase by using the only electric power allows a significant reduction in pollutants in the LTO cycle. However, some limitations of the proposed methodology should be raised: the estimation of hybrid-electric aircraft emissions is not trivial in case of fuel flow lower than current state-of-the art values; in fact, current models do not consider these data, and extrapolations are necessary. Extrapolating data is not a reliable operation when the physical boundaries of the problem are unknown, and this could lead to undetectable errors. The development of novel physics-based models is essential for this purpose.

3.2 CO_2 emissions

This section presents the results for hybrid-electric configurations, designed according to the methodology described in Section 2.2, and optimised to minimise CO_2 emissions, estimated by Eq. (10). Five different scenarios are considered: CO_{2_e}, namely the emission related to the generation of the electricity, and in the following also named 'indirect emissions', is considered varying starting from the scenario based on the current mix of energy sources; in this case CO_{2_e} is equal to 0.42 kg/kWh. For the other scenarios, CO_{2_e} is decreased up to the value of 0 kg/kWh, hence the case of the whole electricity production is based on renewable sources. The intermediate scenarios represent energy mix with an increasing share of renewable-based electric energy production; the selected CO_{2_e} values are [0.42, 0.315, 0.21, 0.105, 0] kg/kWh for the scenario labels named as [V VI III II I]. The values for the different scenarios adopted in this work are extracted from the data reported in [43]. To provide a general overview of the regional applications, four different target ranges are used to design and optimize the different hybrid-electric regional aircraft, namely 200, 400, 600 and 800 nm.

To evaluate the actual effects of the hybrid-electric propulsion in terms of overall climate impact reduction, it is necessary to assess the impact that optimized regional aircraft have in terms of CO_2 emissions reductions compared to the full-thermal state of the art benchmark. Figure 13 reports the outputs of CO_2 emissions for the different five scenarios adopted in this conceptual study; the emissions breakdown is divided between those related to the in-flight fuel combustion and those deriving from electricity production; the CO_2 values related to the thermal competitor are marked by a grey star. Some general but clear conclusions can be extracted by analysing the outcomes presented in Figure 13: *i)* in the current scenario, named 'Scenario V' (see left part of Figure 13), some limited CO_2 emissions reductions can be obtained from the introduction of hybrid-electric propulsion only for very short routes, i.e. 200 nm, whereas for routes longer than 200 nm practically no noticeable benefits are detected. Indeed for progressively increasing design ranges, the optimized configuration minimizing the CO_2 emissions is almost coincident with a full-thermal solution, without thus deviating from the state-of-the-art option. It therefore becomes clear that the indirect contribution of CO_2 emissions has a decisive impact on the actual benefits to be expected from the technological

implementation of electric propulsion; *ii)* in the case of the intermediate scenarios having gradually reducing CO_{2_e} contributions, i.e. 'Scenarios VI, III, II', the reduction in CO_2 emissions resulting from the introduction of hybrid-electric propulsion provides potential gains also for the 400 nm design range. Also in these, scenarios, thus, the indirect contributions to CO_2 emissions prevent to achieve actual benefits for longer ranges; *iii)* finally, in the 'Scenario I', in which electricity production is entirely relying on renewable sources (see right part of Figure 13), a total cut of CO_2 emissions is achieved up to 400 nm, a halving of emissions for the 600 nm design range, while no benefits are obtained for longer flight distances, where again solutions similar to the full-thermal one are found. In this latter case, as there are not indirect emissions, the reason of this result relies on the technological limitations of the batteries, that for longer routes would introduce severe increments of weight, preventing the aircraft from having better performance than a state-of-the-art configuration.

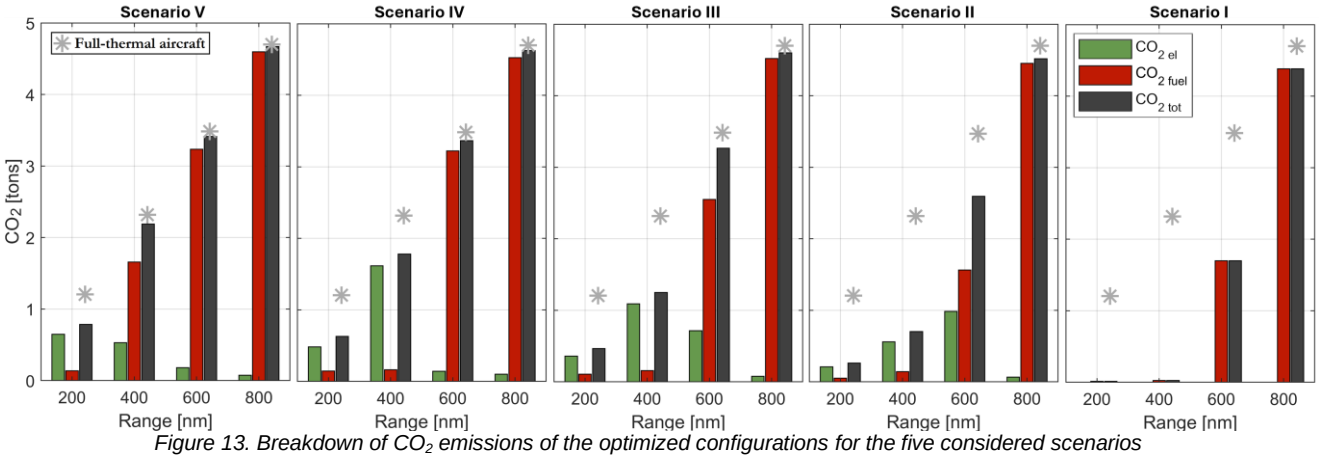

Figure 13. Breakdown of CO_2 emissions of the optimized configurations for the five considered scenarios

In order to better frame the results obtained by the optimiser, and to assess the impact that the considered scenario actually has on the design of the aircraft and its hybrid-electric powertrain, two different outcomes deserve a comment, namely the power supply split during the mission, and the power installed on board and the energy sources used. Considering the first point, the power utilisation during the mission, it is useful to analyse the graphs shown in Figure 14, which depict the time profile of the power supply of both the thermal and the electric chains, for the five different scenarios and the four different ranges considered. As demonstrated in ref. [2], the primary impact on regional hybrid-electric aircraft performance is the thermal/electric power supply split during cruise. The outcomes of ref. [2], in a nutshell, claim that the larger the electric power share supplied at cruise, the higher the reduction in fuel consumption, but also the larger the increase in aircraft weight due to the presence of the heavy battery packs. In addition to these considerations, with the help of the graphs in Figure 14 it is therefore possible to assess how the CO_2 emissions used as an objective function and how the varying contribution of CO_{2_e} have an impact on this result. In the case of Scenario V, it can be seen that electric power is used in cruise only for the 200 nm mission; a small fraction of electric power is supplied in the standard mission for the 400 nm case as well, while the cruises covering longer distances are all accomplished by means of thermal power supply only. It should be noted that the power fractions supplied in the various mission phases are among the design variables managed by the optimiser. These results show that the introduction of hybrid-electric propulsion introduces no benefits in terms of CO_2 emissions, except for very short distances, if the ground-based scenario remains at the status quo in terms of electricity production. Improving the context of indirect emissions, thus moving from Scenario IV towards Scenario I, allows hybrid-electric propulsion to introduce benefits also for the 400 nm route, as seen in the corresponding graphs in Figure 14, where it is evident that the optimiser finds solutions exploiting electric power to accomplish the cruise phase. The situation is different for the 600 nm, where only a fully renewable-based scenario allows the full exploitation of hybrid-electric propulsion to reduce CO_2 emissions. In any scenario, the introduction of this technology leads to no benefits in the case of longer routes, where the supply of thermal power is therefore favoured; it is the low BED of batteries that introduces these limitations.

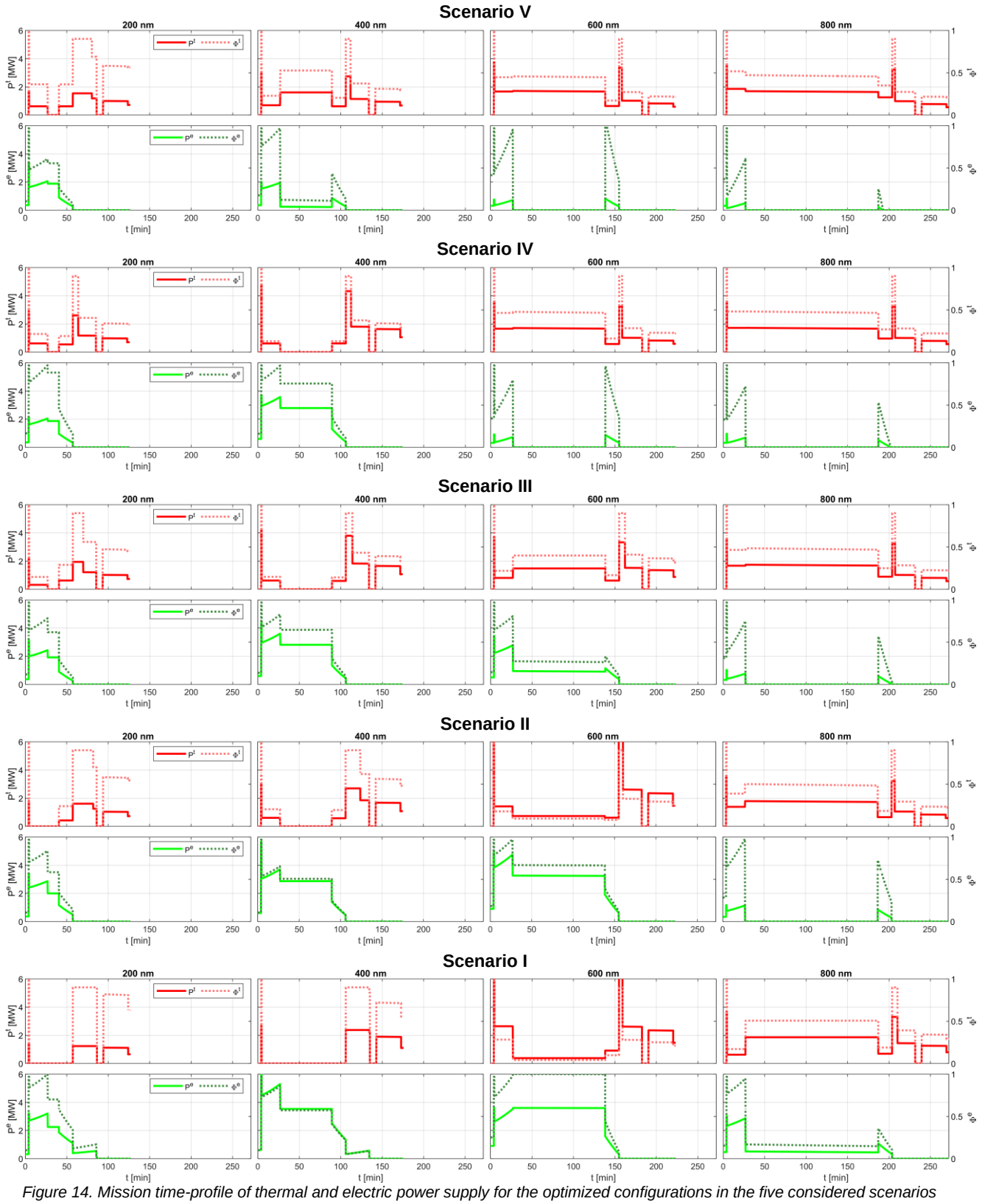

Figure 14. Mission time-profile of thermal and electric power supply for the optimized configurations in the five considered scenarios

Related considerations can be made by commenting on the amount of energy sources mass (batteries and fuel) to be taken on board to accomplish the standard mission of the optimised configurations, as shown in Figure 15. The fully renewable-based Scenario I provide solutions with very high masses of batteries, proving that meeting the energy demand of the flight using electric energy is a favourable solution in terms of reduction of CO_2 emissions; as mentioned before, this applies up to 600 nm, while increases in range would lead to increases in battery mass that would undermine the feasibility of the aircraft. In all scenarios, the optimiser tends to minimise block fuel consumption in the 200 nm and 400 nm reference flight cases. In the current Scenario V, however, only the 200 nm case could introduce some tangible benefit in terms of emission reduction, while partial trade-offs are found in

the intermediate scenarios. It should also be noted that the low BED of the batteries introduces strong penalties in terms of aircraft weight; in the future Scenario I, although benefits can be obtained from an emissions perspective on a 600 nm reference mission, this will only be possible with massive increases in MTOW, see Figure 16. This aspect introduces strong penalties in terms of operating cost and design development, as discussed in ref. [46], and must be strongly taken into account from the early stages of conceptual and feasibility studies for this type of aircraft.

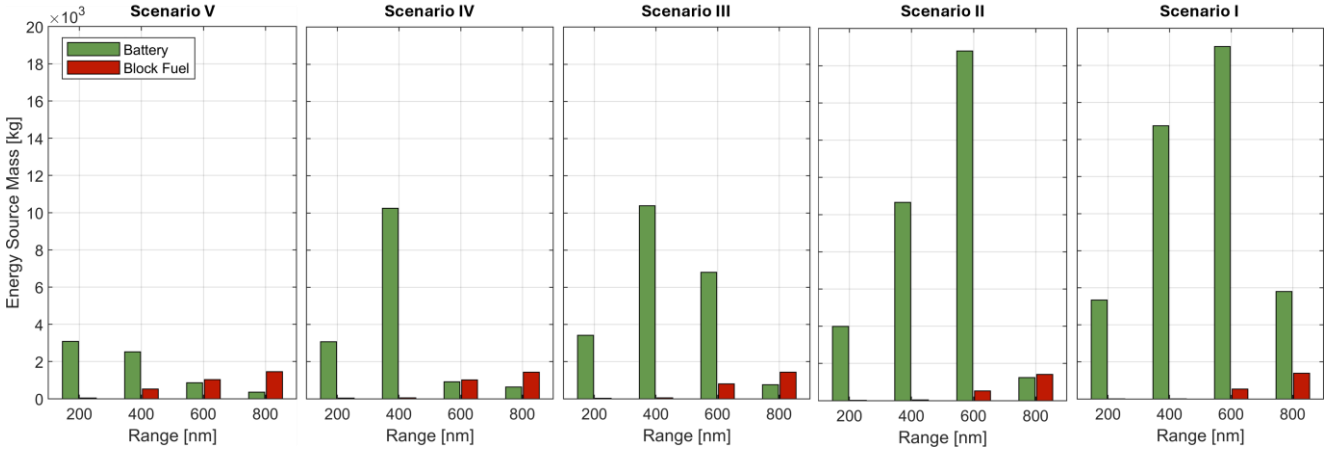

Figure 15. Breakdown of energy sources mass of the optimized configurations for the five considered scenarios

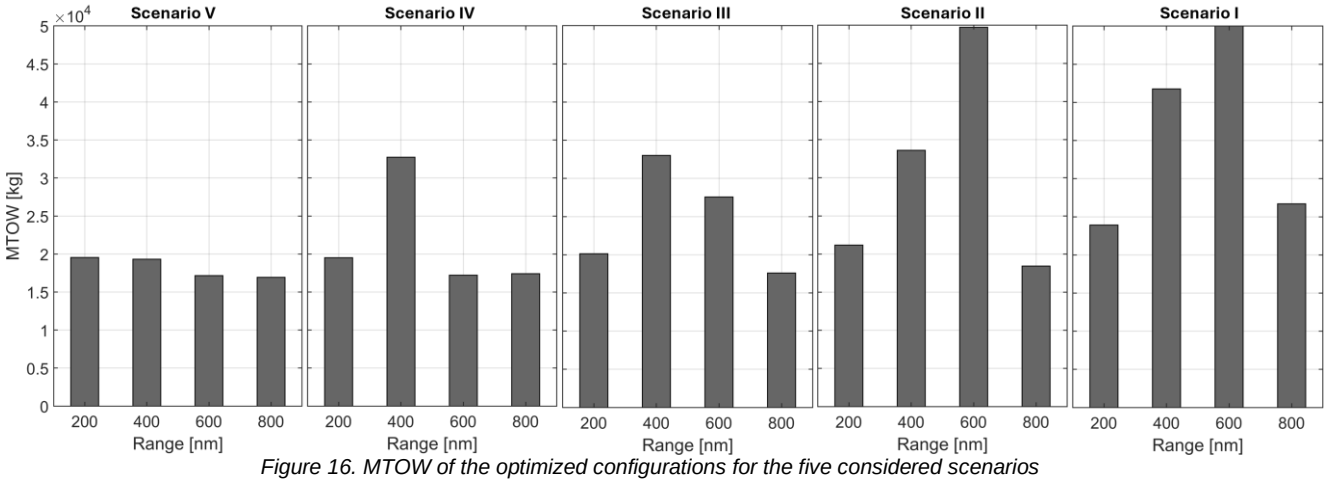

Figure 16. MTOW of the optimized configurations for the five considered scenarios

This overview, even if conceptual, indicates that introducing hybrid-electric propulsion on regional aircraft, considering currently available battery technology forecasts, does not distinctively lead to the necessary environmental targets to be achieved in the near future. Short and extra-short flights are more suitable to achieve CO_2 emissions reductions, but if a significant benefit is to be achieved from the adoption of this technology, a fundamental conversion of the entire energy system is necessary, transitioning swiftly towards a scenario where electricity production relies exclusively on renewable sources.

4. Conclusion

This study addressed the impact of introducing hybrid-electric propulsion for regional transport aircraft in terms of pollutant and greenhouse emissions. This impact is quantitatively assessed by comparing the results with those of a comparable reference full-thermal powered configuration. The models used are based on in-house conceptual aircraft design tools and emissions models and database available in the literature. The main outcomes show that:

- the hybrid-electric aircraft, sized through an optimization procedure that considers block fuel as figure of merit, allows for emissions reductions for all the main pollutants, both over the entire mission and in the LTO cycle;
- the hybrid-electric aircraft, sized through an optimization procedure that has as a figure of merit the minimization of direct (flight-related) and indirect (electricity generation-related) CO_2 emissions, is able to reduce CO_2 emissions in case of ranges shorter than 400 nm, taking into account the current electric power generation scenario. The transition towards an electric

power generation scenario based on renewable sources could provides benefits also for ranges of 600 nm, while the use of hybrid-electric propulsion is ineffective for longer ranges (e.g. 800 nm), due to the weight penalization introduced by batteries.

The proposed results indicate that the hybrid-electric aircraft could have a potential to contribute to the decarbonization of the regional transport sector and to the improvement of local air quality. However, it must be stressed that the development of hybrid-electric aircraft is strictly dependent on the technological development of the electric components, in particular the batteries, and to the improvement of the ground-based scenario. Further developments in this work deal with two different aspects; from a methodological perspective, there is the need to increase the reliability and resolution of predictive emission models in order to obtain increasingly accurate emissions estimates. From an actual impact assessment standpoint, models that translate emissions into metrics directly related to climate change and global warming can be introduced as figures of merit steering the conceptual optimization of hybrid-electric aircraft.

5. Copyright Statement

The authors confirm that they, and/or their company or organization, hold copyright on all of the original material included in this paper. The authors also confirm that they have obtained permission, from the copyright holder of any third party material included in this paper, to publish it as part of their paper. The authors confirm that they give permission, or have obtained permission from the copyright holder of this paper, for the publication and distribution of this paper as part of the ICAS proceedings or as individual off-prints from the proceeding.

References

[1] Brelje B and Martins J. Electric, hybrid, and turboelectric fixed-wing aircraft: A review of concepts, models, and design approaches. *Progress in Aerospace Sciences*, Vol. 104, 2018. https://doi.org/10.1016/j.paerosci.2018.06.004

[2] Abu Salem K, Palaia G, and Quarta AA. Review of hybrid-electric aircraft technologies and designs: critical analysis and novel solutions. *Progress in Aerospace Sciences*, Vol. 141, 2023. https://doi.org/10.1016/j.paerosci.2023.100924

[3] Barzkar A and Ghassemi M. Components of Electrical Power Systems in More and All-Electric Aircraft: A Review. *IEEE Transactions on Transportation Electrification*, Vol. 8, No. 4, pp. 4037-4053, 2022. Doi: 10.1109/TTE.2022.3174362.

[4] Moebs N, Eisenhut D, Windels E, van der Pols J and Strohmayer A. Adaptive Initial Sizing Method and Safety Assessment for Hybrid-Electric Regional Aircraft. *Aerospace*, Vol. 9, 2022. https://doi.org/10.3390/aerospace9030150

[5] Papathakis KV, Burkhardt PA, David WE and Alaric MS. Safety Considerations for Electric, Hybrid-Electric, and Turbo-Electric Distributed Propulsion Aircraft Testbeds. *53rd AIAA/SAE/ASEE Joint Propulsion Conference*, Atlanta, GA, 10-12 July 2017. https://doi.org/10.2514/6.2017-5032

[6] Trainelli L, Salucci F, Riboldi CED, Rolando A and Bigoni F. Optimal Sizing and Operation of Airport Infrastructures in Support of Electric-Powered Aviation. *Aerospace*, Vol. 8, 2021. https://doi.org/10.3390/aerospace8020040

[7] Jordan C, Harris T, Krah K, Morris J, Li X and Cary S. Impacts of Regional Air Mobility and Electrified Aircraft on Airport Electricity Infrastructure and Demand. Golden, CO: National Renewable Energy Laboratory. NREL/TP-5R00- 84176. 2023. https://www.nrel.gov/docs/fy23osti/84176.pdf

[8] Viswanathan V, Epstein AH, Chiang YM et al. The challenges and opportunities of battery-powered flight. *Nature*, Vol. 601, pp 519–525, 2022. https://doi.org/10.1038/s41586-021-04139-1

[9] Palaia G, Abu Salem K and Quarta AA. Parametric Analysis for Hybrid–Electric Regional Aircraft Conceptual Design and Development. Appl. Sci, Vol. 13, 2023. https://doi.org/10.3390/app131911113

[10] Abu Salem K, Palaia G, Quarta AA and Chiarelli MR. Medium-Range Aircraft Conceptual Design from a Local Air Quality and Climate Change Viewpoint. *Energies*, Vol. 16, 2023. https://doi.org/10.3390/en16104013

[11] Guzhva VS, Curtis T and Borodulin V. Market analysis for small and mid-size commercial turboprop aircraft. *International Journal of Aviation Management*, Vol. 2, 2015. Doi:10.1504/IJAM.2015.072376

[12] Prapotnik BA, Kamnik R, Marksel M and Božičnik S. Market and Technological Perspectives for the New Generation of Regional Passenger Aircraft. *Energies*, Vol. 12, 2019. https://doi.org/10.3390/en12101864

[13] Brooker P. Civil aircraft design priorities: Air quality? climate change? noise? *Aeronaut. J.*, Vol. 110, pp 517–532, 2006. https://doi.org/10.1017/S0001924000001408

[14] Stettler MEJ, Eastham S and Barrett SRH. Air quality and public health impacts of UK airports. Part I: Emissions. *Atmos. Environ.*, Vol. 45, 2011. https://doi.org/10.1016/j.atmosenv.2011.07.012

[15] Parker R. From blue skies to green skies: Engine technology to reduce the climate-change impacts of aviation. *Technol. Anal. Strat. Manag*., Vol. 21, 2009. https://doi.org/10.1080/09537320802557301

[16] Lee DS, Pitari G, Grewe V, Gierens K, Penner JE, Petzold A, Prather MJ, Schumann U, Bais A, Berntsen T, Iachetti D, Lim LL and Sausen R. Transport impacts on atmosphere and climate: Aviation. *Atmospheric Environment*, Vol. 44, 2010. https://doi.org/10.1016/j.atmosenv.2009.06.005

[17] Brazzola N, Patt A and Wohland J. Definitions and implications of climate-neutral aviation. *Nat. Clim. Chang*. Vol. 12, pp 761–767, 2022. https://doi.org/10.1038/s41558-022-01404-7

[18] Rogelj J. Disentangling the effects of CO2 and short-lived climate forcer mitigation. *Proceedings of the National Academy of Sciences*, Vol. 111, pp 16325-16330. https://doi.org/10.1073/pnas.1415631111

[19] Proesmans PJ and Vos R. Airplane design optimization for minimal global warming impact. *Journal of Aircraft*, Vol. 59, pp 1363-1381, 2022. https://doi.org/10.2514/1.C036529

[20] Tasca AL, Cipolla V, Abu Salem K and Puccini M. Innovative Box-Wing Aircraft: Emissions and Climate Change. *Sustainability*, Vol. 13, 2021. https://doi.org/10.3390/su13063282

[21] Filippone A and Parkes B. Evaluation of commuter airplane emissions: A European case study. *Transportation Research Part D: Transport and Environment*, Vol. 98, 2021. https://doi.org/10.1016/j.trd.2021.102979

[22] Filippone A and Bojdo N. Statistical model for gas turbine engines exhaust emissions. *Transportation Research Part D: Transport and Environment*, Vol. 59, pp 451-463, 2018. https://doi.org/10.1016/j.trd.2018.01.019

[23] Palaia G, Zanetti D, Abu Salem K et al. THEA-CODE: A design tool for the conceptual design of hybrid electric aircraft with conventional or unconventional airframe configurations. *Mechanics and Industry*, Vol. 22, 2021. https://doi.org/10.1051/meca/2021012

[24] Palaia G. Design and performance assessment methodologies for box-wing hybrid-electric aircraft from urban to regional transport applications. *Ph.D. Thesis*, University of Pisa, 2022. https://etd.adm.unipi.it/t/etd-11092022-150110/

[25] Rizzo E and Frediani A. Application of Optimisation Algorithms to Aircraft Aerodynamics. *Variational Analysis and Aerospace Engineering*, Springer Optimization and Its Applications, Vol 33, Springer, New York, NY, 2009. https://doi.org/10.1007/978-0-387-95857-6_23

[26] Abu Salem K, Palaia G, Cipolla V et al. Tools and methodologies for box-wing aircraft conceptual aerodynamic design and aeromechanic analysis. *Mechanics & Industry*, Vol. 22, 2021. https://doi.org/10.1051/meca/2021037

[27] Drela, M and Youngren H. AVL 3.36 User Primer, Online software manual, 2017. https://perma.cc/R35R-W29F

[28] D. Raymer, *Aircraft Design: A Conceptual Approach*, 6th Edition, American Institute of Aeronautics and Astronautics, AIAA, 2018, ISBN: 9781600869112

[29] Drela M and Youngren H. XFOIL 6.9 user primer, Online software manual, 2001. https://web.mit.edu/drela/Public/web/xfoil/

[30] Cipolla V, Abu Salem K, Palaia G, Binante V and Zanetti D. A DoE-based approach for the implementation of structural surrogate models in the early stage design of box-wing aircraft. *Aerospace Science and Technology*, Vol. 117, 2021. https://doi.org/10.1016/j.ast.2021.106968

[31] Palaia G, Abu Salem K, Cipolla V, Zanetti D and Binante, V. A DoE-based scalable approach for the preliminary structural design of Box-Wing aircraft from regional to medium range categories. *AIAA SciTech Forum*, National Harbor, USA, 23-27 January 2023. https://doi.org/10.2514/6.2023-2082

[32] Wells DP, Horvath BL and McCullers LA. The Flight Optimization System Weights Estimation Method. *NASA Tech. Rep*. 2017. Available online: https://ntrs.nasa.gov/citations/20170005851

[33] Sforza PM. *Commercial airplane design principles*, Elsevier: Amsterdam, The Netherlands, 2014, ISBN 9780124199538

[34] Fioriti M. Adaptable conceptual aircraft design model. *Advances in Aircraft and Spacecraft Science*, Vol. 1, pp 043-067, 2014. http://dx.doi.org/10.12989/aas.2014.1.1.043

[35] Palaia G and Abu Salem, K. Mission Performance Analysis of Hybrid-Electric Regional Aircraft. *Aerospace*, Vol. 10, 2023. https://doi.org/10.3390/aerospace10030246

[36] Wilkerson JT et al. Analysis of emission data from global commercial aviation: 2004 and 2006. *Atmos. Chem. Phys*., Vol. 10, pp. 6391–6408, 2010. https://doi.org/10.5194/acp-10-6391-2010

[37] Kapadia ZZ et al. Impacts of aviation fuel sulfur content on climate and human health. *Atmos. Chem. Phys.*, Vol. 16, pp. 10521–10541, 2016. Doi:10.5194/acp-16-10521-2016

[38] DuBois D and Paynter GC. "Fuel Flow Method2" for Estimating Aircraft Emissions. *Journal of Aerospace*, Vol. 115, pp. 1-14, 2006. https://doi.org/10.4271/2006-01-1987.

[39] Baughcum S.L. et al. Scheduled Civil Aircraft Emission Inventories for 1992: Database Development and Analysis. *NASA Contractor Report 4700*. https://ntrs.nasa.gov/api/citations/19960038445/downloads/19960038445.pdf

[40] Avions Transport Regional. ATR: the optimum choice for a friendly environment. *Modern Transport and Environment*, 2001. https://web.archive.org/web/20160808173542/http://web.fc.fi/data/files/ATR_TheOptimumChoice.pdf

[41] Schaefer M.,Bartosch S. Overview on fuel flow correlation methods for the calculation of NOx, CO and HC emissions and their implementation into aircraft performance software. DLR Institut für Antriebstechnik, Report number: IB-325-11-13.

[42] Overton J. The Growth in Greenhouse Gas Emissions from Commercial Aviation. Environmental and Energy Study Institute, 2022. Available online: https://www.eesi.org/papers/view/fact-sheet-the-growth-in-greenhouse-gas-emissions-from-commercial-aviation

[43] Hoelzen J, Liu Y, Bensmann B, Winnefeld C, Elham A, Friedrichs J and Hanke-Rauschenbach R. Conceptual Design of Operation Strategies for Hybrid Electric Aircraft. *Energies*, Vol. 11, No. 217, pp 1-26, 2018. https://doi.org/10.3390/en11010217

[44] Hainsch K, Göke L, Kemfert C, Oei PY and Hirschhausen CV. European green deal: Using ambitious climate targets and renewable energy to climb out of the economic crisis. *DIW Weekly Report*, Vol. 10, pp 303–310, 2020. https://doi.org/10.18723/DIW_DWR:2020-28-1

[45] Kougias I, Taylor N, Kakoulaki, G, and Jäger-Waldau A. The role of photovoltaics for the European green deal and the recovery plan. *Renewable and Sustainable Energy Reviews*, Vol. 144, 2021. https://doi.org/10.1016/j.rser.2021.111017.

[46] Abu Salem K, Palaia G and Quarta AA. Impact of Figures of Merit Selection on the Hybrid-Electric Regional Aircraft Performance Analysis. *Energies*, Vol. 16, 2023. https://doi.org/10.3390/en16237881